e-ISSN: 2954-4440

ARTICLE

Current Topics in Agronomic Science

https://doi.org/10.5154/r.ctasci.2025.05.12

English version

Effects of nitrogen deficiency on chlorophyll expression and synthesis in tomato

Juan Pablo Ledesma-Valladolid[1]*; Mayra Isabel Niño-González[1]; Guadalupe Xóchitl Malda-Barrera[2]; Juan Ramiro Pacheco-Aguilar[1]; Gerardo Manuel Nava-Morales[1]*; Edmundo Mateo Mercado-Silva[1]*

[1]Universidad Autónoma de Querétaro, Facultad de Química, Santiago de Querétaro, Querétaro, México.
[2]Universidad Autónoma de Querétaro, Facultad de Ciencias Naturales, Santiago de Querétaro, Querétaro, México.

Article history:
Received: April 21, 2025
Accepted: October 31, 2025
Published online:
December 22, 2025
***Corresponding author:**
jpledesma95@gmail.com,
gerardomnava@gmail.com,
mercado501120@gmail.com

Abstract

Chlorophyll synthesis plays an important role in maintaining photosynthetic efficiency, as well as in regulating plant development and tolerance to abiotic stress conditions such as nitrogen deficiency under nutrient management regimes. It has been demonstrated that the chlorophyll synthesis pathway maintains a mutually regulated dynamic relationship with the intracellular nitrogen assimilation pathway. This dynamic is controlled by the activity of enzymes such as uroporphyrinogen III methyltransferase (UPM1), which is key to tolerance under nitrogen-deficiency stress and to maintaining optimal levels of chlorophyll synthesis. The objective of this study was to identify the genes involved in the chlorophyll synthesis pathway and UPM1, characterize their functions, evaluate their gene expression levels *in silico*, and quantify their total chlorophyll in tomato under nitrogen-deficient conditions. The results indicate that the proteins involved in the chlorophyll synthesis pathway and their functions are conserved in tomato plants. Moreover, nitrogen deficiency reduced the gene expression levels of *SlHEMD* and *SlUPM1* (36 ans 49 %, respectively), as well as total chlorophyll content by 20 %.

Keywords: Comparative genomics, bioinformatics, *Solanum lycopersicum*.

Introduction

Photosynthesis is the most important biochemical mechanism for biological organisms. It is estimated that between 90-95 % of the biomass produced in plants comes directly from photosynthesis (Bag et al., 2020; Chen et al., 2023; Makino & Sage, 2007). Photosynthesis is divided into two main stages: the light-dependent reactions and the Calvin-Benson cycle (Shimizu et al., 2015). In the light-dependent reactions, the absorption of photons from solar energy induces electron transport across the thylakoid membrane within the chloroplasts. This electron gradient promotes the synthesis of energy in the form of ATP and NADPH (Pietrzykowska et al., 2014). Subsequently, this energy is used by the reactions of the Calvin-Benson cycle for carbon dioxide fixation and the synthesis of organic compounds (Smith et al., 2024).

The maintenance of photosynthetic capacity depends on the conformation of photosystems I and II. The photosystems are composed of the reaction centers and the light-harvesting complexes (LhcA/B) (Croce & van Amerongen, 2013; Gao et al., 2018; Nelson & Yocum, 2006; van Amerongen & Croce, 2013). The light-harvesting complexes consist of a series of proteins known as Chlorophyll a/b binding Protein. These proteins serve as binding sites for the chlorophylls, which together carry out the absorption and transfer of energy to the reaction center of the photosystems, sub-

Please cite this article as follows (APA 7): Ledesma-Valladolid, J. P., Niño-González, M. I., Malda-Barrera, G. X., Pacheco-Aguilar, J. R., Nava-Morales, G. M., & Mercado-Silva, E. M. (2025). Effects of nitrogen deficiency on chlorophyll expression and synthesis in tomato. *Current Topics in Agronomic Science, 5*. e2512. https://doi.org/10.5154/r.ctasci.2025.05.12

sequently initiating the electron gradient (Croce & van Amerongen, 2013; Gao et al., 2018; Nelson & Yocum, 2006; van Amerongen & Croce, 2013).

The chlorophyll biosynthetic pathway is an essential component for the proper assembly of the photosystems and for the maintenance of photosynthetic capacity (Mao et al., 2025). This pathway is coordinated by a series of reactions that are divided into four main sub-stages (Chatterjee et al., 2015). The first stage enables the synthesis of aminolevulinic acid from glutamic acid as the precursor. The second set of reactions promotes the synthesis of uroporphyrinogen III using the 5-aminolevulinic acid generated in the previous stage as the precursor. The third stage involves the synthesis of protoporphyrin IX from uroporphyrinogen III as the precursor. Finally, the fourth stage comprises the synthesis of chlorophyll *a* from protoporphyrin IX (Wu, et al., 2019b).

Nitrogen is the most important macronutrient in crop nutrition management (Krapp, 2015). In plant nutrition, nitrogen is primarily supplied in the forms of nitate (NO^-_3) and ammonium (NH^+_4), and to a lesser extent as amino acids and short-chain peptides (Zayed et al., 2023). Once taken up by the root systems, these compounds (NO^-_3 and NH^+_4) are transported to the foliar system through the vascular tissue. In the leaves, they are metabolized via the intracellular nitrogen assimilation pathway, which involves enzymes such as nitrate reductase (NR), nitrate reductase (NiR), glutamate synthase (GOGAT), and glutamine synthetase (GS) (Gilad, et al., 2025). Factors such as the nitrogen supply rate, the NO^-_3/NH^+_4 ratio in plant nutrition, and the activity of the intracellular assimilation enzymes regulate the capacity for glutamic acid synthesis, thereby affecting chlorophyll synthesis and the photosynthetic capacity of crops (Roosta et al., 2025; Guo et al., 2007).

Several studies have demonstrated a reduction in chlorophyll content as well as a decrease in photosynthetic capacity in models subjected to nitrogen-deficient conditions (Cetner et al., 2017; Ferreira et al., 2016; Lu et al., 2021). Under nitrogen deficiency, a reduction in the expression levels of genes associated with enzymes of the chlorophyll synthesis pathways, such as *HEMA1*, *HEMA2*, *HEMB1*, *HEMC*, *HEMD* and *HEMF* has been observed. These results were correlated with decreased levels of 5-aminolevulinic acid and total chlorophyll, as well as with a decrease in the expression levels of genes associated with enzymes of the intracellular nitrogen assimilation pathway, including *NR*, *NiR*, *GOGAT* and *GS* (Wen et al., 2019a).

It has been shown that the dynamics of the interaction between the chlorophyll biosynthesis pathway and the intracellular nitrogen assimilation pathway may be regulated by the activity of uroporphyrinogen III methyltransferase (UPM1) (Garai et al., 2016). UPM1 plays an important role in the synthesis of the prosthetic group siroheme. Siroheme is an integral component of nitrite reductase as a prosthetic group. This group is synthesized in the chloroplasts using uroporphyrinogen III as a precursor (Tanaka, et al., 2011). UPM1 appears to play a vital role in nitrogen metabolism through the assembly of nitrite reductase, which contributes to the regulation of glutamic acid levels in the chloroplast. This metabolic interplay, in turn, contributes to the regulation of chlorophyll synthesis and the photosynthetic capacity of crops (Garai & Tripathy, 2018).

Understanding the impact of low nitrogen supply on the expression levels of enzymes in the chlorophyll synthesis pathway and UPM1 is crucial for clarifying crop responses to nutritional stress. The objective of this study was to identify the genes involved in the chlorophyll synthesis pathway and UPM1, characterize their functions, evaluate their gene expression levels *in silico*, and assess chlorophyll synthesis capacity in tomato under nitrogen-deficient conditions.

Materials and Methods

Identification and characterization of the genes and proteins of the chlorophyll synthesis pathway and UPM1

To identify the amino acid and nucleotide sequences (CDS; coding sequence, and genomic sequence) involved in the chlorophyll synthesis pathway and UPM1 in tomato, the sequences were first identified in *Arabidopsis thaliana*, which was used as a reference model. These sequences were retrieved from the TAIR database (https://www.arabidopsis.org). Subsequently, a comparative genomic analysis was performed using the BLASTP tool (https://blast.ncbi.nlm.nih.gov/) against the complete protein collection (CDS translations+PDB+SwissProt+PIR+PRF) archived in GenBank (834,777,505 sequences; as of November 2024). The search and comparison were restricted to *Solanum lycopersicum* (taxid:4081). The following parameters were applied for the analysis: percent identity (≥ 80 %), percent coverage (≥ 90 %) and E-value ($1e^{-10}$). The accession numbers with the best results were used to retrieve the amino acid and nucleotide sequences (CDS and genomic sequences) for tomato deposited in GenBank. (https://www.ncbi.nlm.nih.gov/). Using the collected sequences, the following characteristics were estimated: protein molecular weight (MW-P), isoelectric point (pI), amino acid sequence length (AA-L), and protein subcellular localization through the Expasy tool (https://web.expasy.org/cgi-bin/protparam/protparam), WoLF PSORT (https://www.genscript.com/wolf-psort.html) and Cell-PLoc 2.0 (http://www.csbio.sjtu.edu.cn/bioinf/plant-multi/). The nucleotide sequences were used to determine the number of exons and introns, as well as the chromosomal location of the genes identified in *A. thaliana* and tomato (Lan et al., 2022).

Multiple sequence alignment and phylogenetic analysis of amino acid sequences

To identify intra- and interspecific homology, as well as to understand the evolutionary relationships among the protein sequence identified in *A. thaliana* and tomato, a multiple sequence alignment analysis was performed. The ClustalW method was used for this purpose, applying the default parameters in Mega XI. Subsequently, the phylogenetic tree was constructed using the Neighbor-Joining tree, using the Jones-Taylor Thornton model with 1 000 bootstrap replicates. Finally, the iTOL tool (https://itol.embl.de/) was used to generate a high-quality schematic representation (Lan et al., 2022).

Structural analysis of genes and proteins in the chlorophyll synthesis pathway and UPM1

To verify the functionality of the protein and genomic sequence identified in tomato, a structural analysis of these sequences was performed. Exons and introns of the genomic sequence were analyzed and identified using the Gene Structure Display Server (GSDS) (https://gsds.gao-lab.org/). In addition, conserved protein motifs were identified using the MEME plataform (https://meme-suite.org/meme/tools/meme) and InterPro (https://www.ebi.ac.uk/interpro/). The diagrams were generated using the TBtools platform (v2.096, https://github.com/CJ-Chen/TBtools-II) (Lan et al., 2022).

In silico analysis of gene expression in the chlorophyll synthesis pathway and UPM1 in tomato under low-nitrogen conditions

To determine the effect of low-nitrogen conditions on the *in silico* expression levels of the genes identified in tomato, Illumina RNA-seq data were analyzed from the NCBI-GEO database (https://www.ncbi.nlm.nih.gov/gds). The data corresponded to two different treatments: control treatment (CT) and low-nitrogen treatment (LNT). Gene accession numbers were used to assess the effect of each treatment on their expression levels. The results were reported as FPKM (Fragments per kilobase of exon per million).

Plant material and treatments

The present study was conducted in commercial greenhouses under a hydroponic production system using coconut fiber as the substrate. The greenhouses had the following characteristics: gothic-type design, polyethylene flooring and covering, north-south orientation, and passive ventilation systems with front windows. Sixteen days after germination, the seedlings were grafted using "Maxifort" rootstocks and transplanted into the substrate in hydroponic production systems. The plants were subjected to two treatments: a control treatment (CT) and a low-nitrogen treatment (LNT). For the control treatment, a drip irrigation system was used to supply Hoagland solution with the following composition: NO^-_3 (17.54 mmol), NH^+_4 (1.91 mmol), H_2PO_4 (3.79 mmol), SO^-_4 (4.2 mmol), K^+ (9.65 mmol), Ca^+_2 (8.41 mmol), Mg^+_2 (2.3 mmol), B^+_3 (148.01 mmol), Cl^- (10.2 mmol), Cu^+_2 (1.58 mmol), Fe^-_2 (55.34 mmol), Mn^+_4 (13.29 mmol) and Zn^+ (12.54 mmol). For the LNT treatment, a drip irrigation system was also used to supply Hoagland solution with the following composition: NO^-_3 (12.3 mmol), NH^+_4 (0.96 mmol), H_2PO_4 (1.34 mmol), SO^-_4 (3.2 mmol), K^+ (7.57 mmol), Ca^+_2 (3.87 mmol), Mg^+_2 (1.69 mmol), B^+_3 (83.26 mmol), Cl^- (4.6 mmol), Cu^+_2 (1.1 mmol), Fe^-_2 (43.34 mmol), Mn^+_4 (9.1 mmol) and Zn^+ (8.41 mmol). The electrical conductivity and pH of the Hoagland solution for the CT were 4.35 $mS \cdot cm^{-1}$ and 5.62, respectively, while for LNT the electrical conductivity and pH were 2.54 $mS \cdot cm^{-1}$ and 5.15, respectively. The crop production cycle extended from week 10 to week 50 of development following transplanting. During this period, 15 plants per treatment were randomly selected for sampling.

Sampling collection

Leaf samples (n=15) were randomly collected throughout the greenhouse. The eighth compound leaf was selected for sampling, with leaf numbering initiated from the uppermost leaf. Samples were placed in sterile bags and kept at 4 °C, then flash-frozen in liquid nitrogen and stored at -81 °C.

Total Chlorophyll Content

Total chlorophyll content was estimated following the methodology described by Wu et al., (2019); Xi et al., (2021) and Zhong et al., (2017). A total of 200 mg of fresh leaf tissue was weighed, and 25 mL of an alcohol-acetone extraction solution 1:1 (v/v) was added. The mixture was homogenized at 10 000 rpm for 1 minute using an Ultra-Turrax (IKA, T-25D). The homogenate was then centrifuged at 10 000 rpm for 2 minutes at 4 °C. The supernatant was recovered, and absorbance was measured at 663 and 645 nm. Total chlorophyll content was expressed as $mg*g^{-1}$ FW. The following equation was used:

Total Chlorophyll Content ($mg*g^{-1}$ PF) =
(20.2)(ABS 645 nm) - (8.02)(ABS 663 nm)

Results and Discussion

Identification and physicochemical characterization of genes and proteins involved in the chlorophyll synthesis pathway and UPM1

In this study, twenty-six genes and proteins involved in the chlorophyll synthesis pathway were identified in *A. thaliana*. Additionally, a single gene responsible for

UPM1 expression was identified. In tomato, 19 genes and proteins associated with the chlorophyll synthesis pathway were identified through comparative genomic analysis using the BLASTP tool, with *A. thaliana* as the reference model, and one gene responsible for UPM1 expression was also found. The physicochemical characteristics of the identified genes and proteins, including coding sequence length (CDS length, (LS-CDS), number of exons (NE), chromosomal location, amino acid sequence length (LS-AA), protein molecular weight (kDa) (PM-P), protein isoelectric point (PI), and subcellular localization, are systematically described in Table 1. For the chlorophyll synthesis pathways genes in *A. thaliana*, LS-CDS was 938 pb (*AtHEMD*) to 2 282 pb (*AtCHLD*). In tomato, the identified genes showed LS-CDS values ranging from 908 pb (*SlHEMD*) to 2 300 pb (*SlCHLD*). Regarding chromosomal localization, in *A. thaliana*, chromosome 1 showed the highest gene density (GD) with eight genes, while chromosome 2 had the lowest GD with three genes. In tomato, chromosomes 4 and 10 showed the highest GD, each containing ten genes. The protein sequences identified in *A. thaliana* showed amino acid sequence lengths, PM-P and PI ranging from 312 aa (*AtCHLM*) – 1 381 aa (*AtCHLH*), de 33 796 kDa (*AtCHLM*) – 153 574 kDa (*AtCHLH*) and 5.26 (*AtCHLD*) - 9.49 (*AtNOL*). In tomato, the identified proteins showed LS-AA from 302 aa (*SlHEMD*) to 1 381 aa (*SlCHLH*), PM-P from 32 359 kDa (*SlHEMD*) to 153 688 kDa (*SlCHLH*) and PI from 5.28 (*SlCHLD*) to 9.42 (*SlPORB*). Subcellular localization prediction indicated that the proteins in both species are localized to chloroplast, including specific components such as thylakoid membranes and the stroma (Table 1).

Multiple sequence alignment and phylogenetic analysis of animo acid sequences

The evolutionary relationships of the proteins identified in *A. thaliana* and tomato were evaluated both intra- and interspecifically. Phylogenetic analysis revealed a close relationship between the proteins identified in both species (Figure 1), with homologous proteins from tomato and *A. thaliana* clustering within the same clade. Similarly, UPM1 from both species was successfully grouped into a single clade. The sequences identified in tomato showed high homology relative to the proteins identified in *A. thaliana*. Multiple sequence alignment showed an average homology of approximately 78 % between the proteins of the two species. The lowest homology was observed for HEMD at 63.97 % whereas the highest was for CHLH at 86.19 %. The high degree of homology between the two species indicates the presence of orthologous genes with conserved functionality, which likely arose from speciation events during the evolutionary history of tomato and *A. thaliana* (Liu et al., 2023; Mao et al., 2022; Xi et al., 2022; Xia et al.,

Table 1. Identification of genes and proteins of the chlorophyll synthesis pathway and their physicochemical characteristics.

Species	Gene name	Protein GenBank ID	Gen GenBank ID	Protein length (aa)	Protein molecular weight (kDa)	Isoelectric point	CDS length (pb)	Number of exons	Chromosomal location	Subcellular localization	
										Cell-PLoc 2.0	WoLF PSORT
A. thaliana	*AtHEMA1*	NP_176125.1	NM_104609.4	543	59,515	7.95	1,631	3	1	Chloroplast	Chloroplast
A. thaliana	*AtHEMA2*	NP_172465.1	NM_100868.3	530	58,292	8.82	1,592	3	1	Chloroplast	Chloroplast
A. thaliana	*AtHEMA3*	NP_180683.1	NM_128681.3	524	58,691	8.78	1,574	3	2	Chloroplast	Chloroplast
A. thaliana	*AtGSA1*	NP_201162.1	NM_125752.4	474	50,370	6.42	1,424	3	5	Chloroplast	Chloroplast
A. thaliana	*AtGSA2*	NP_190442.1	NM_114732.5	472	50,142	7.01	1,418	4	3	Chloroplast	Chloroplast
A. thaliana	*AtHEMB1*	NP_177132.1	NM_105642.4	430	46,690	6.96	1,292	13	1	Chloroplast	Chloroplast
A. thaliana	*AtHEMB2*	NP_175085.1	NM_103545.2	406	44,878	8.39	1,221	10	1	Chloroplast	Thylakoid membrane
A. thaliana	*AtHEMC*	NP_196445.1	NM_120911.4	382	41,043	8.75	1,148	5	5	Chloroplast	Thylakoid membrane
A. thaliana	*AtHEMD*	NP_565625.1	NM_128211.4	321	34,225	7.81	965	9	2	Chloroplast	Thylakoid membrane
A. thaliana	*AtHEME1*	NP_850587.1	NM_180256.2	418	46,254	6.64	1,256	6	3	Chloroplast	Chloroplast
A. thaliana	*AtHEME2*	NP_181581.1	NM_129611.5	394	43,580	8.29	1,184	6	2	Chloroplast	Thylakoid membrane
A. thaliana	*AtHEMF*	NP_171847.4	NM_100230.7	386	43,796	6.24	1,160	8	1	Chloroplast	Chloroplast
A. thaliana	*AtHEMG1*	NP_192078.1	NM_116399.4	537	57,695	9.13	1,613	9	4	Chloroplast	Thylakoid membrane
A. thaliana	*AtCHLH*	NP_196867.1	NM_121366.4	1381	153,574	5.8	4,145	5	5	Chloroplast	Chloroplast
A. thaliana	*AtCHLD*	NP_563821.2	NM_100725.4	760	83,284	5.26	2,282	15	1	Chloroplast	Stroma
A. thaliana	*AtCHLI1*	NP_193583.1	NM_117962.3	424	46,270	6.08	1,274	3	4	Chloroplast	Stroma
A. thaliana	*AtCHLI2*	NP_199405.2	NM_123961.4	418	46,098	5.36	1,256	3	5	Chloroplast	Stroma

Table 1. Identification of genes and proteins of the chlorophyll synthesis pathway and their physicochemical characteristics. (*cont.*)

Species	Gene name	Protein GenBank ID	Gen GenBank ID	Protein length (aa)	Protein molecular weight (kDa)	Isoelectric point	CDS length (pb)	Number of exons	Chromosomal location	Subcellular localization	
										Cell-PLoc 2.0	WoLF PSORT
A. thaliana	*AtCHLM*	NP_194238.1	NM_118640.3	312	33,796	7.68	938	3	4	Chloroplast	Thylakoid membrane
A. thaliana	*AtCRD1*	NP_191253.1	NM_115553.4	409	47,631	8.55	1,229	5	3	Chloroplast	Thylakoid membrane
A. thaliana	*AtDVR*	NP_197367.1	NM_121871.3	417	45,893	7.47	1,253	1	5	Chloroplast	Thylakoid membrane /Stroma
A. thaliana	*AtPORA*	NP_200230.1	NM_124799.4	405	43,863	9.42	1,217	4	5	Chloroplast	Chloroplast
A. thaliana	*AtPORB*	NP_194474.1	NM_118879.4	401	43,359	9.23	1,205	5	4	Chloroplast	Chloroplast
A. thaliana	*AtPORC*	NP_171860.1	NM_100243.4	401	43,883	9.18	1,205	5	1	Chloroplast	Chloroplast
A. thaliana	*AtCAO*	NP_175088.1	NM_103548.5	536	60,331	7.96	1,610	8	1	Chloroplast	Chloroplast
A. thaliana	*AtNOL*	NP_568145.1	NM_120572.3	348	38,149	9.49	1,046	13	5	Chloroplast	Chloroplast
A. thaliana	*AtCHLG*	NP_190750.1	NM_115041.4	387	41,881	8.52	1,163	14	3	Chloroplast	Stroma
S. lycopersicum	*SlHEMA1*	XP_004238036.1	XM_004237988.4	544	59,342	8.37	1,634	3	4	Chloroplast	Chloroplast
S. lycopersicum	*SlGSA*	NP_001234690.2	NM_001247761.2	482	51,500	6.53	1,448	3	4	Chloroplast	Chloroplast
S. lycopersicum	*SlHEMB*	XP_004245301.1	XM_004245253.4	430	46,836	6.36	1,292	14	8	Chloroplast	Chloroplast
S. lycopersicum	*SlHEMD*	XP_010320354.1	XM_010322053.4	302	32,359	8.19	908	10	4	Chloroplast	Chloroplast
S. lycopersicum	*SlHEME*	XP_010327114.1	XM_010328812.4	420	45,984	6.47	1,262	6	10	Chloroplast	Chloroplast
S. lycopersicum	*SlHEMF*	XP_004248412.2	XM_004248364.5	399	44,717	5.8	1,199	8	10	Chloroplast	Chloroplast
S. lycopersicum	*SlHEMG1*	NP_001335308.1	NM_001348379.1	558	60,446	8.98	1,676	8	1	Chloroplast	Chloroplast
S. lycopersicum	*SlCHLH*	XP_004236610.1	XM_004236562.5	1381	153,688	5.93	4,145	5	4	Chloroplast	Chloroplast
S. lycopersicum	*SlCHLD*	XP_004236627.1	XM_004236579.5	766	83,918	5.28	2,300	15	4	Chloroplast	Chloroplast
S. lycopersicum	*SlCHLI*	XP_004248139.1	XM_004248091.5	427	46,434	6.07	1,283	3	10	Chloroplast	Chloroplast
S. lycopersicum	*SlCHLM*	XP_004235845.2	XM_004235797.5	327	35,532	6.96	983	2	3	Chloroplast	Chloroplast
S. lycopersicum	*SlCRD1*	NP_001332768.1	NM_001345839.1	404	47,185	8.99	1,214	5	10	Chloroplast	Chloroplast
S. lycopersicum	*SlDVR*	XP_010321210.1	XM_010322908.4	420	46,086	6.41	1,262	2	1	Chloroplast	Chloroplast
S. lycopersicum	*SlPORA*	XP_004251852.1	XM_004251804.5	397	42,812	9.19	1,193	5	12	Chloroplast	Chloroplast
S. lycopersicum	*SlPORB*	NP_001304903.1	NM_001317974.1	395	42,611	9.42	1,187	5	10	Chloroplast	Chloroplast
S. lycopersicum	*SlPORC*	NP_001296970.1	NM_001310041.1	399	43,199	9.27	1,199	5	7	Chloroplast	Chloroplast
S. lycopersicum	*SlCAO*	XP_004250311.1	XM_004250263.5	535	60,237	7.54	1,607	9	11	Chloroplast	Chloroplast
S. lycopersicum	*SlNOL*	XP_010321272.1	XM_010322970.4	346	37,925	9.22	1,040	13	5	Chloroplast	Chloroplast
S. lycopersicum	*SlCHLG*	XP_004246318.1	XM_004246270.4	369	40,038	8.26	1,109	15	9	Chloroplast	Chloroplast

* pb; base pairs, kDa; kilodaltons, aa; amino acids

2023). In the case of *A. thaliana*, multiple sequence alignment enabled the identification of two or three isoforms for HEMA, GSA, HEMB, HEME and CHLI. For HEMA (HEMA1, HEME2 and HEMA3), as shown in Table 1 and Figure 1, the alignment revealed high homology among the three isoforms (68-81 %). The isoform groups for GSA (GSA1 and GSA2), HEMB (HEMB1 and HEMB2), HEME (HEME1 and HEME2) and CHLI (CHLI1 and CHLI2) had homology levels of 90, 65, 51 and 83 % respectively. The POR protein family (PORA, PORB y PORC) showed high homology among its members (77-87 %). These results suggest that gene duplication events have occurred throughout the evolutionary history of *A. thaliana*, leading to the generation of paralogous genes with conserved functionality (Liu et al., 2023; Mao et al., 2022; Xi et al., 2022; Xia et al., 2023). Finally, the amino acid sequences of UPM1 also had high homology (75 %).

Structural analysis of genes and proteins in the chlorophyll synthesis pathway and UPM1

The structural characteristics of the genes and proteins identified in tomato were analyzed. Exon (CDS)/Intron structural analysis revealed considerable divergence

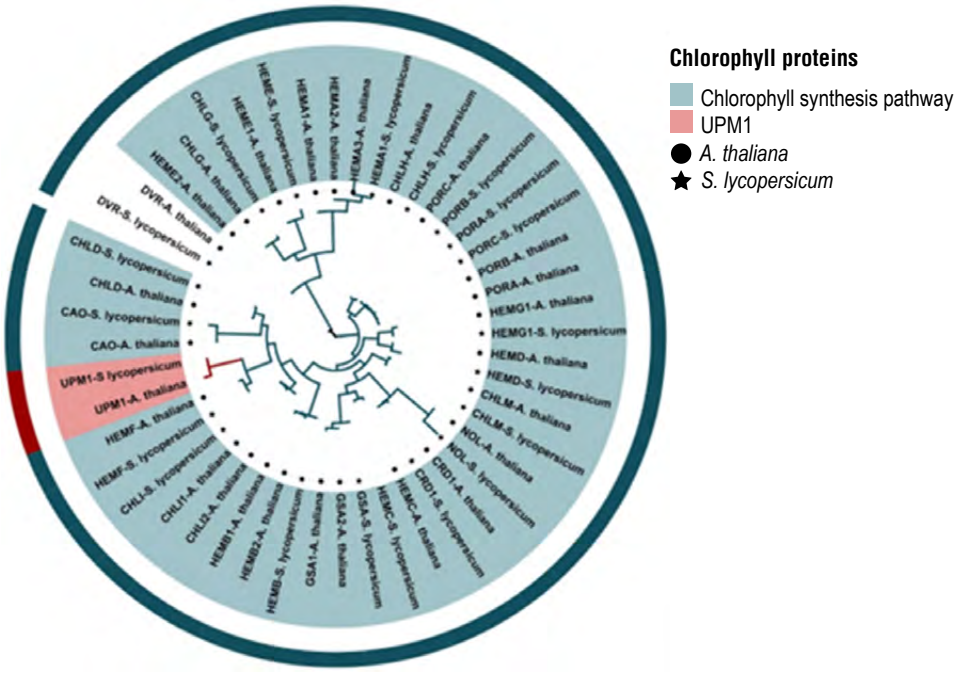

*The phylogenetic tree was constructed using the neighbor-joining method with 1000bootstrap replicates and fitted to the Jones-Taylor Thorton model.

Figure 1. Phylogenetic analysis of amino acid sequences identified in tomato and *Arabidopsis thaliana*.

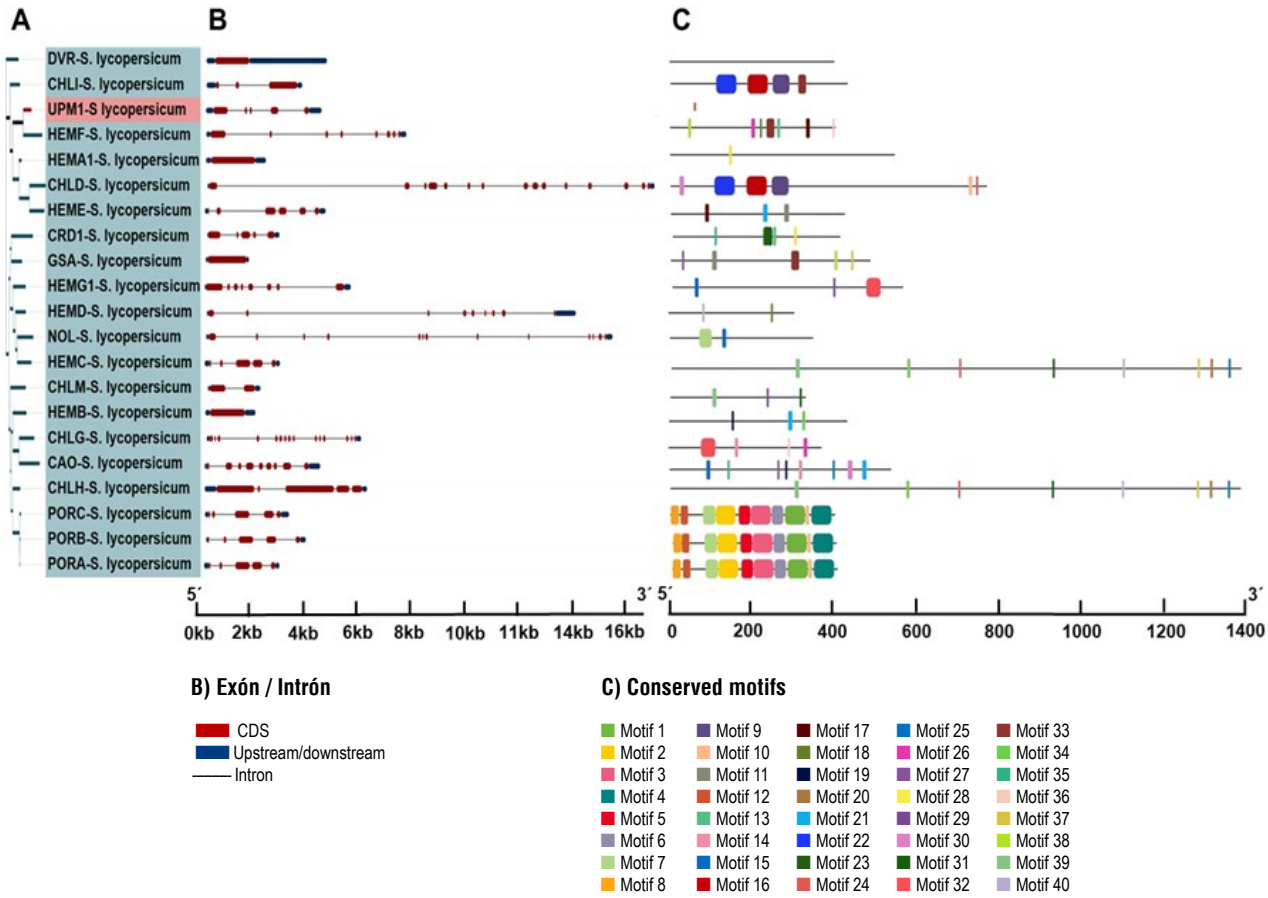

Figure 2. Phylogenetic analysis of sequences identified in tomato, generated using the Neighbor-joining method. (B) Structural genomic analysis of CDS and UTR sequences, represented by red and blue boxes, respectively, and introns represented by solid black lines. (C) Analysis of conserved protein motifs in the chlorophyll synthesis pathway and UPM1 in tomato.

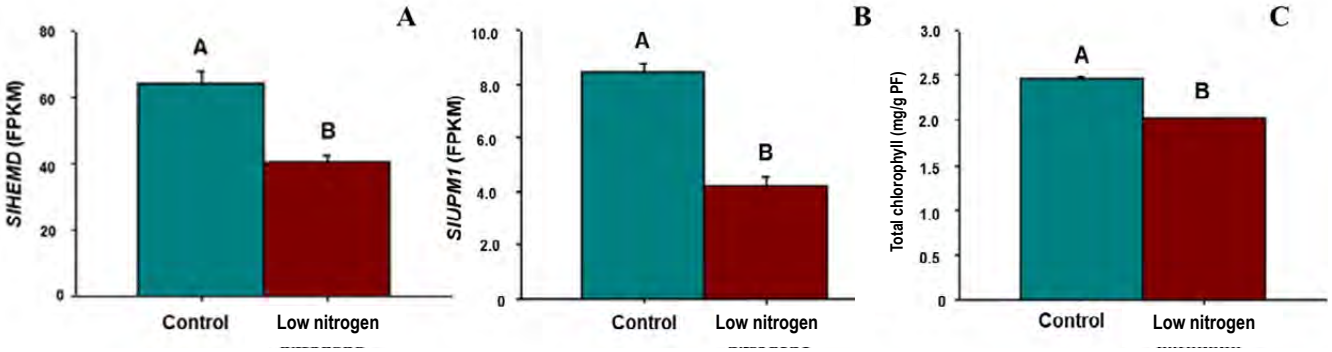

* Genomic expression data was obtained from NCBI-GEO database and are expressed as FPKM (Fragments per Kilobase of transcript per Million mapped reads).

** The data is presented as mean ± standard error (*n*=15). Bars with the same letter are not statistically different according to Tukey's test. The "Control" and "Low nitrogen" treatments are represented by green and red bars, respectively. The graphs were generated using SigmaPlot 11.

Figure 3. (A and B) Comparison of *SlHEMD* and *SlUPM1*. (c) Comparison of total chlorophyll synthesis in leaves.

among the identified genes (Table 1 and Figure 2B). In this study, the number of exons ranged from 2 (*SlDVR* and *SlCHLM*) to 15 (*SlCHLD* and *SlCHLG*). These results suggest that intron insertion and loss events have occurred throughout the evolutionary history of tomato. These structural changes may also be associated with alterations in the functionality of the proteins encoded by these genes (Liu et al., 2023). The structural analysis of the identified proteins and their corresponding genomic sequences revealed considerable structural divergence. In this study, up to 40 conserved protein motifs were identified in the amino acid sequences. In contrast, the UPM1 protein sequence showed only a single conserved motif in its structure (Figure 2C). The high number of conserved motifs is associated with the observed variability, which is also reflected in the number of introns and exons in the genomic sequences (Figure 2 B).

In silico expresión levels of *SlHEMD*, *SlUPM1* and total chlorophyll content

The *in silico* expression levels of *SlHEMD* and *SlUPM1* were analyzed under LNT and CT conditions. The results showed an approximately 36 % reduction in *SlHEMD* transcript level under LNT conditions (Figure 3A). For *SlUPM1*, the results also showed a ≈49 % decrease in transcript level under LNT (Figure 3B). Total chlorophyll content (TCC) under LNT conditions showed a 20 % (Figure 3C). UPM1 is an essential component for the optimal functioning of the intracellular nitrogen assimilation pathway (Garai & Tripathy, 2018). It also promotes the synthesis of the prosthetic group siroheme, which is part of the structure of nitrite reductase (Garai & Tripathy, 2018). These findings suggest that reduced *SlUPM1* transcript levels lead to lower efficiency in intracellular nitrogen metabolism; and a decreased intracellular nitrogen metabolic rate is associated with a reduced capacity to synthesize intermediate metabolites such as glutamic acid. As the primary precursor for chlorophyll synthesis, glutamic acid shortage contributes to the decline in *SlHEMD* transcript levels as well as the reduction in total chlorophyll synthesis. Several studies have documented the impact of nitrogen deficiency on the expression levels of enzymes in the chlorophyll synthesis pathway. Choi et al., (2016); Wen et al., (2019) and Yoneda et al., (2016) reported a decrease in the expression of *MdHEMA1, MdHEMA2, MdHEMB1, MdHEMD, SechlL* and *SechlN*. These reductions were associated with decreased synthesis of intermediate metabolites in the chlorophyll synthesis pathway, such as 5-amino levulinic acid and uroporphyrinogen III. Wen et al., (2019) reported reduced levels of *MdNiR*.

Finally, overexpression of *AtUPM1* was associated with increased expression levels of *AtNII* and *AtNIA2* (291 and 280 %, respectively). These results correlated with higher expression levels of *AtUROD*, *AtCHLH*, *AtPORC*, as well as increases of 50, 97, 79 and 25 %, respectively.

Conclusions

The results show that the proteins of the chlorophyll synthesis pathway and their functionality are conserved in tomato plants. Furthermore, a severe impact is observed under nitrogen-deficiency stress, resulting in reduced expression of *SlHEMD* and *SlUPM1* and decreased chlorophyll synthesis capacity. These findings highlight the important role of UPM1 under these conditions in regulating chlorophyll synthesis.

References

Bag, P., Chukhutsina, V., Zhang, Z., Paul, S., Ivanov, A. G., Shutova, T., Croce, R., Holzwarth, A. R., & Jansson, S. (2020). Direct energy transfer from photosystem II to photosystem I confers winter sustainability in Scots Pine. *Nature Communications*, *11*(1), 6388. https://doi.org/10.1038/s41467-020-20137-9

Cetner, M. D., Kalaji, H. M., Goltsev, V., Aleksandrov, V., Kowalczyk, K., Borucki, W., & Jajoo, A. (2017). Effects of nitrogen-

deficiency on efficiency of light-harvesting apparatus in radish. *Plant Physiology and Biochemistry*, *119*, 81-92. https://doi.org/10.1016/j.plaphy.2017.08.016

Chatterjee, A., & Kundu, S. (2015). Revisiting the chlorophyll biosynthesis pathway using genome scale metabolic model of Oryza sativa japonica. *Scientific Reports*, *5*(1), 14975. https://doi.org/10.1038/srep14975

Chen, L., Yang, W., Liu, S., Meng, Y., Zhu, Z., Liang, R., Cao, K., Xie, Y., & Li, X. (2023). Genome-wide analysis and identification of light-harvesting chlorophyll *a*/b binding (LHC) gene family and BSMV-VIGS silencing *TaLHC86* reduced salt tolerance in wheat. *International Journal of Biological Macromolecules*, *242*, 124930. https://doi.org/10.1016/j.ijbiomac.2023.124930

Choi, S. Y., Park, B., Choi, I.-G., Sim, S. J., Lee, S.-M., Um, Y., & Woo, H. M. (2016). Transcriptome landscape of Synechococcus elongatus PCC 7942 for nitrogen starvation responses using RNA-seq. *Scientific Reports*, *6*(1), 30584. https://doi.org/10.1038/srep30584

Croce, R., & van Amerongen, H. (2013). Light-harvesting in photosystem I. *Photosynthesis Research*, *116*(2-3), 153-166. https://doi.org/10.1007/s11120-013-9838-x

Ferreira, V. S., Pinto, R. F., & Sant'Anna, C. (2016). Low light intensity and nitrogen starvation modulate the chlorophyll content of *Scenedesmus dimorphus*. *Journal of Applied Microbiology*, *120*(3), 661-670. https://doi.org/10.1111/jam.13007

Gao, J., Wang, H., Yuan, Q., & Feng, Y. (2018). Structure and Function of the Photosystem Supercomplexes. *Frontiers in Plant Science*, *9*, 357. https://doi.org/10.3389/fpls.2018.00357

Garai, S., & Tripathy, B. C. (2018). Alleviation of Nitrogen and Sulfur Deficiency and Enhancement of Photosynthesis in Arabidopsis thaliana by Overexpression of Uroporphyrinogen III Methyltransferase (UPM1). *Frontiers in Plant Science*, *8*, 2265. https://doi.org/10.3389/fpls.2017.02265

Garai S., Joshi N. C., & Tripathy B.C. (2016). Phylogenetic analysis and photoregulation of siroheme biosynthesis genes: uroporphyrinogen III methyltransferase and sirohydrochlorin ferrochelatase of Arabidopsis thaliana. *Physiol Mol Biol Plants* 22(3):351-359. https://doi.org/10.1007/s12298-016-0363-1

Gilad G., Sapir O., Hipsch M., Waiger D., Ben-Ari J., Zeev BB, Zait Y., Lampl N., & Rosenwasser S. (2025). Nitrogen Assimilation Plays a Role in Balancing the Chloroplastic Glutathione Redox Potential Under High Light Conditions. *Plant Cell Environ*. 48(5):3559-3572. https://doi.org/10.1111/pce.15368

Guo S., Zhou Y., Shen Q., & Zhang F. (2007). Effect of ammonium and nitrate nutrition on some physiological processes in higher plants - growth, photosynthesis, photorespiration, and water relations. *Plant Biol* 9(1):21-9. https://doi.org/10.1055/s-2006-924541

Krapp A. (2015). Plant nitrogen assimilation and its regulation: a complex puzzle with missing pieces. Curr Opin *Plant Biol*. 25:115-22. https://doi.org/10.1016/j.pbi.2015.05.010

Lan, Y., Song, Y., Zhao, F., Cao, Y., Luo, D., Qiao, D., Cao, Y., & Xu, H. (2022). Phylogenetic, Structural and Functional Evolution of the LHC Gene Family in Plant Species. International Journal of Molecular Sciences, 24(1), 488. https://doi.org/10.3390/ijms24010488

Liu, J., Wang, C., Peng, J., Ju, J., Li, Y., Li, C., & Su, J. (2023). Genome-wide investigation and expression profiles of the NPF gene family provide insight into the abiotic stress resistance of Gossypium hirsutum. Frontiers in Plant Science, 14, 1103340. https://doi.org/10.3389/fpls.2023.1103340

Lu, L., Zhang, Y., Li, L., Yi, N., Liu, Y., Qaseem, M. F., Li, H., & Wu, A. M. (2021). Physiological and Transcriptomic Responses to Nitrogen Deficiency in Neolamarckia cadamba. Frontiers in Plant Science, 12, 747121. https://doi.org/10.3389/fpls.2021.747121

Makino, A., & Sage, R. F. (2007). Temperature Response of Photosynthesis in Transgenic Rice Transformed with 'Sense' or 'Antisense' rbcS. Plant and Cell Physiology, 48(10), 1472-1483. https://doi.org/10.1093/pcp/pcm118

Mao, P., Run, Y., Wang, H., Han, C., Zhang, L., Zhan, K., Xu, H., & Cheng, X. (2022). Genome-Wide Identification and Functional Characterization of the Chloride Channel TaCLC Gene Family in Wheat (Triticum aestivum L.). Frontiers in Genetics, 13, 846795. https://doi.org/10.3389/fgene.2022.846795

Mao H. T., Pang X, Li T., Qin Y., Zhang Z. W., Yuan S., Yuan M., Brestic M., & Chen Y. E. (2025). Chlorophyll b is essential for the growth, photoprotection, and photosystem I assembly in wheat. Plant J.;123(4):e70442. https://doi.org/10.1111/tpj.70442

Nelson, N., & Yocum, C. F. (2006). Structure and function of photosystems i and ii. Annual Review of Plant Biology, 57(1), 521-565. https://doi.org/10.1146/annurev.arplant.57.032905.105350

Pietrzykowska, M., Suorsa, M., Semchonok, D. A., Tikkanen, M., Boekema, E. J., Aro, E.-M., & Jansson, S. (2014). The Light-Harvesting Chlorophyll a/b Binding Proteins Lhcb1 and Lhcb2 Play Complementary Roles during State Transitions in Arabidopsis. The Plant Cell, 26(9), 3646-3660. https://doi.org/10.1105/tpc.114.127373

Roosta, H. R., Estaji, A., Khadivi, A., & Shams M. (2025). Balanced ammonium–nitrate nutrition enhances photosynthetic efficiency, micronutrient homeostasis, and antioxidant networks via ROS signaling in Glycyrrhiza glabra across soil and soilless systems. Sci Rep 15, 25404 . https://doi.org/10.1038/s41598-025-11181-w

Shimizu, R., Dempo, Y., Nakayama, Y., Nakamura, S., Bamba, T., Fukusaki, E., & Fukui, T. (2015). New Insight into the Role of the Calvin Cycle: Reutilization of CO2 Emitted through Sugar Degradation. Scientific Reports, 5(1), 11617. https://doi.org/10.1038/srep11617

Slattery, R. A., VanLoocke, A., Bernacchi, C. J., Zhu, X.-G., & Ort, D. R. (2017). Photosynthesis, Light Use Efficiency, and Yield of Reduced-Chlorophyll Soybean Mutants in Field Conditions. Frontiers in Plant Science, 8. https://doi.org/10.3389/fpls.2017.00549

Smith, K., Strand, D. D. & Walker, B. J. (2024) Evaluating the contribution of plant metabolic pathways in the light to the ATP: NADPH demand using a meta-analysis of isotopically non-stationary metabolic flux analyses. Photosynth Res 161, 177–189. https://doi.org/10.1007/s11120-024-01106-5

Tanaka R., Kobayashi K., & Masuda T. (2011). Tetrapyrrole Metabolism in Arabidopsis thaliana. *The Arabidopsis Book* (9). https://doi.org/10.1199/tab.0145

van Amerongen, H., & Croce, R. (2013). Light harvesting in photosystem II. Photosynthesis Research, 116(2-3), 251-263. https://doi.org/10.1007/s11120-013-9824-3

Wen, B., Li, C., Fu, X., Li, D., Li, L., Chen, X., Wu, H., Cui, X., Zhang, X., Shen, H., Zhang, W., Xiao, W., & Gao, D. (2019a). Effects of nitrate

deficiency on nitrate assimilation and chlorophyll synthesis of detached apple leaves. Plant Physiology and Biochemistry, 142, 363-371. https://doi.org/10.1016/j.plaphy.2019.07.007

Wu, Y., Li, Q., Jin, R., Chen, W., Liu, X., Kong, F., Ke, Y., Shi, H., & Yuan, J. (2019). Effect of low-nitrogen stress on photosynthesis and chlorophyll fluorescence characteristics of maize cultivars with different low-nitrogen tolerances. Journal of Integrative Agriculture, 18(6), 1246-1256. https://doi.org/10.1016/S2095-3119(18)62030-1

Wu, Y., Liao, W., Dawuda, M.M., Hu, l., & Yu, J. (2019). 5-Aminolevulinic acid (ALA) biosynthetic and metabolic pathways and its role in higher plants: a review. Plant Growth Regul 87, 357–374 (2019). https://doi.org/10.1007/s10725-018-0463-8

Xi, Y., Hu, W., Zhou, Y., Liu, X., & Qian, Y. (2022). Genome-Wide Identification and Functional Analysis of Polyamine Oxidase Genes in Maize Reveal Essential Roles in Abiotic Stress Tolerance. Frontiers in Plant Science, 13, 950064. https://doi.org/10.3389/fpls.2022.950064

Xi, Y., Yin, L., Chi, Z. & Luo, G. (2021). Characterization and RNA-seq transcriptomic analysis of a Scenedesmus obliqnus mutant with enhanced photosynthesis efficiency and lipid productivity. Scientific Reports, 11(1), 11795. https://doi.org/10.1038/s41598-021-88954-6

Xia, J., Wang, Y., Zhang, T., Pan, C., Ji, Y., Zhou, Y., & Jiang, X. (2023). Genome-wide identification, expression profiling, and functional analysis of ammonium transporter 2 (AMT2) gene family in cassava (Manihot esculenta crantz). Frontiers in Genetics, 14, 1145735. https://doi.org/10.3389/fgene.2023.1145735

Yoneda, A., Wittmann, B. J., King, J. D., Blankenship, R. E., & Dantas, G. (2016). Transcriptomic analysis illuminates genes involved in chlorophyll synthesis after nitrogen starvation in Acaryochloris sp. CCMEE 5410. Photosynthesis Research, 129(2), 171-182. https://doi.org/10.1007/s11120-016-0279-1

Zayed O, Hewedy O. A, Abdelmoteleb A, Ali M, Youssef M. S, Roumia A. F, Seymour D, & Yuan Z. C. (2023). Nitrogen Journey in Plants: From Uptake to Metabolism, Stress Response, and Microbe Interaction. Biomolecules 13(10):1443. https://doi.org/10.3390/biom13101443

Zhong, C., Cao, X., Hu, J., Zhu, L., Zhang, J., Huang, J., & Jin, Q. (2017). Nitrogen Metabolism in Adaptation of Photosynthesis to Water Stress in Rice Grown under Different Nitrogen Levels. Frontiers in Plant Science, 8, 1079. https://doi.org/10.3389/fpls.2017.01079